VISUALIZATION OF Nd^{3+}-DOPED LaF_3 NANOPARTICLES FOR NEAR INFRARED BIOIMAGING VIA UPCONVERSION LUMINESCENCE AT MULTIPHOTON EXCITATION MICROSCOPY

Ryabova A.V.[1], Keevend K.[2], Tsolaki E.[3], Bertazzo S.[3], Pominova D.V.[1], Romanishkin I.D.[1], Grachev P.V. [1], Makarov V.I.[1], Burmistrov I.A.[4], Vanetsev A.S.[1,6], Orlovskaya E.O.[1], Baranchikov A.E.[5], Rähn M.[6], Sildos I.[6], Sammelselg V.[6], Loschenov V.B.[1], Orlovskii Y.V.[1,6]
[1]General Physics Institute of the Russian Academy of Sciences, Moscow, Russia
[2]Swiss Federal Laboratories for Materials Science and Technology (Empa), St. Gallen, Switzerland
[3]University College London (UCL), London, United Kingdom
[4]Lomonosov Moscow State University, Moscow, Russia
[5]Kurnakov Institute of General and Inorganic Chemistry RAS, Moscow, Russia
[6]Institute of Physics, University of Tartu, Tartu, Estonia

Abstract

Recent developments in the field of biophotonics facilitate the raise of interest to inorganic nanoparticles (NPs) doped with Nd^{3+} ions, because of their near-infrared (NIR) absorption. These NPs are interesting bioimaging probes for deep tissue visualization, while they can also act as local thermometers in biological tissues. Despite the good possibilities for visualization of NPs with Nd^{3+} ions in NIR spectral range, difficulties arise when studying the cellular uptake of these NPs using commercially available fluorescence microscopy systems, since the selection of suitable luminescence detectors is limited. However, Nd^{3+} ions are able to convert NIR radiation into visible light, showing upconversion properties. In this paper we found optimal parameters to excite upconversion luminescence of Nd^{3+}:LaF_3 NPs in living cells and to compare the distribution of the NPs inside the cell culture of human macrophages THP-1 obtained by two methods. Firstly, by detecting the upconversion luminescence of the NPs in VIS under NIR multiphoton excitation using laser scanning confocal microscopy and secondly, using transmission electron microscopy.

Keywords: Nd^{3+}-doped nanoparticles, near-infrared, upconversion luminescence, multiphoton excitation, laser scanning confocal microscopy.

For citations: Ryabova A.V., Keevend K., Tsolaki E., Bertazzo S., Pominova D.V., Romanishkin I.D., Grachev P.V., Makarov V.I., Burmistrov I.A., Vanetsev A.S., Orlovskaya E.O., Baranchikov A.E., Rähn M., Sildos I., Sammelselg V., Loschenov V.B., Orlovskii Yu.V. Visualization of Nd^{3+}-doped LaF_3 nanoparticles for near infrared bioimaging via upconversion luminescence at multiphoton excitation microscopy, *Biomedical Photonics*, 2018, T. 7, No. 1, pp. 4–12.

Contacts: Ryabova A.V., e-mail: nastya.ryabova@gmail.com

ВИЗУАЛИЗАЦИЯ НАНОЧАСТИЦ LaF_3, ДОПИРОВАННЫХ Nd^{3+}, ДЛЯ БИОИМИДЖИНГА В БЛИЖНЕМ ИНФРАКРАСНОМ ДИАПАЗОНЕ ПО АП-КОНВЕРСИОННОЙ ЛЮМИНЕСЦЕНЦИИ ПРИ МИКРОСКОПИИ С МУЛЬТИФОТОННЫМ ВОЗБУЖДЕНИЕМ

А.В. Рябова[1], K. Keevend[2], E. Tsolaki[3], S. Bertazzo[3], Д.В. Поминова[1], И.Д. Романишкин[1], П.В. Грачев[1], В.И. Макаров[1], И.А. Бурмистров[4], А.С. Ванецев[1,6], Е.О. Орловская[1], А.Е. Баранчиков[5], M. Rähn[6], I. Sildos[6], V. Sammelselg[6], В.Б. Лощенов[1], Ю.В. Орловский[1,6]
[1]Институт общей физики им. А.М. Прохорова РАН, Москва, Россия
[2]Swiss Federal Laboratories for Materials Science and Technology (Empa), Switzerland
[3]University College London (UCL), London, United Kingdom
[4]Московский государственный университет им. М.В. Ломоносова, Москва, Россия
[5]Институт общей и неорганической химии им. Н.С. Курнакова РАН, Москва, Россия
[6]Institute of Physics, University of Tartu, Estonia

Резюме

Последние разработки в области биофотоники способствуют повышению интереса к неорганическим наночастицам (НЧ), допированным ионами Nd^{3+}, из-за их поглощения в ближнем инфракрасном (БИК) спектральном диапазоне. Эти НЧ являются перспективными зондами для глубокой визуализации тканей, в то же время они могут служить локальными термометрами в биологических тканях. Несмотря на хорошие возможности визуализации НЧ с ионами Nd^{3+} в БИК спектральном диапазоне, при изучении внутриклеточного распределения этих НЧ с использованием коммерчески доступных флуоресцентных микроскопических систем возникают трудности из-за ограниченности выбора подходящих детекторов люминесценции. Однако, ионы Nd^{3+} способны преобразовывать БИК излучение в видимый свет, демонстрируя ап-конверсионные свойства. В этой работе мы определили оптимальные параметры для возбуждения ап-конверсионной люминесценции НЧ Nd^{3+}: LaF_3 в живых клетках и сравнили распределение НЧ внутри клеток культуры человеческих макрофагов THP-1, полученное двумя методами. Во-первых, путем регистрации ап-конверсионной люминесценции НЧ в видимом диапазоне при многофотонном возбуждении в БИК диапазоне спектра с использованием лазерной сканирующей конфокальной микроскопии и, во-вторых, с использованием просвечивающей электронной микроскопии.

Ключевые слова: наночастицы, допированные Nd^{3+}, ближний инфракрасный спектральный диапазон, ап-конверсионная люминесценция, мультифотонное возбуждение, лазерная сканирующая конфокальная микроскопия.

Для цитирования: Рябова А.В., Keevend K., Tsolaki E., Bertazzo S., Поминова Д.В., Романишкин И.Д., Грачев П.В., Макаров В.И., Бурмистров И.А., Ванецев А.С., Орловская Е.О., Баранчиков А.Е., Rähn M., Sildos I., Sammelselg V., Лощенов В.Б., Орловский Ю.В. Визуализация наночастиц LaF_3, допированных Nd^{3+}, для биоимиджинга в ближнем инфракрасном диапазоне по ап-конверсионной люминесценции при микроскопии с мультифотонным возбуждением // Biomedical Photonics. – 2018. – Т. 7, № 1. – С. 4–12.

Контакты: Рябова А.В., e-mail: nastya.ryabova@gmail.com

Introduction

Optical imaging plays an important role in biomedical research and clinical diagnosis. Obtaining optical images from the depth of biological tissue is a serious scientific task, since biotissue is heterogeneous and has a strong scattering and absorption by various components. NIR spectral region (700-950 nm) is most suitable for excitation during *in vivo* visualization due to minimal absorption by biotissue.

In the last decade a lot of attention has been paid to the inorganic NPs containing rare-earth ions, as a promising class of nanomaterials for biophotonics. The advantages of rare-earth ions as luminescent labels include narrow-band radiation, a large spectral shift between the excitation and emission wavelengths, which is characteristic for the up- and down-conversion, long luminescence lifetime, high photostability of materials and low toxicity, minimization of autofluorescence of biological tissues by time resolved fluorescence spectroscopy and the greatest penetration depth when NPs are excited in the NIR spectral range [1]. Rare-earth ions can be excited through multiple electronic states, and, due to internal conversion, can show luminescence bands in a wide range of UV, VIS, and IR including the second biological window of optical transparency in short-wavelength infrared (SWIR) [2].

NPs doped with Nd^{3+} ions, are increasingly considered as an improvement for the upconversion system of ion pair, one of which is the sensitizer Yb^{3+}, with the possibility of excitation by 800 nm [3-6]. The absorption cross section of Nd^{3+} at 808 nm is $1.2\times10^{-19}cm^2$, about ten times larger than that of Yb^{3+}at 980 nm [7], which is conducive to improve the efficiency of upconversion process through Nd-sensitizing [8]. Also, the Nd^{3+}-containing NPs are perspective as bioimaging probes [9] and non-invasive contactless fluorescence temperature sensors [10]. The water colloids of Nd^{3+}:LaF_3 NPs synthesized by hydrothermal microwave treatment have already shown themselves to be excellent fluorescent agents for bioimaging in the NIR spectral range [11].

Despite the good possibilities for visualization of NPs with Nd^{3+} ions in NIR spectral range, difficulties arise when studying the cell uptake of these NPs using the methods of common VIS fluorescent microscopy that are associated with the selection of suitable detectors of luminescence [12-14]. Fortunately, the materials doped with Nd^{3+} ions can convert NIR radiation into VIS, while Nd^{3+} ions can simultaneously act as both sensitizers and activators of upconversion. In this case, the probability of emission in VIS is higher at high pump densities, when high-energy levels of most of the Nd^{3+} ions in one NP are populated [15].

The present work demonstrates the visualization of the intracellular distribution of Nd^{3+}:LaF_3NPs by laser scanning confocal microscopy with multiphoton excitation in the NIR spectral range by pumping into the $^4F_{5/2}$, $^2H_{9/2}$ (795 nm) and $^4F_{7/2}$, $^2S_{3/2}$ (738 nm) levels of Nd^{3+} and detection of two-photon and three-photon upconversion luminescence in the VIS range.

Materials and methods

Synthesis of Nd^{3+}-doped lanthanum trifluoride NPs

We use water based hydrothermal microwave treatment (HTMW) synthetic approaches to crystalline 4% Nd^{3+}:LaF_3 NPs. NPs with such Nd^{3+} doping concentration

is selected as having the highest NIR luminescence brightness. For the synthesis of LaF_3 NPs doped with 4% Nd^{3+} ions, 0.48 mM $La(NO_3)_3 \cdot 6H_2O$ and 0.02 mM $Nd(NO_3)_3 \cdot 5H_2O$ were dissolved in 15 ml deionized water (dH_2O). The solution of rare-earth salts was added dropwise to the 5 mM NH_4F solution in 25 ml dH_2O under vigorous stirring. To improve the dispersibility of the obtained NPs, 1 g of biocompatible surfactant polyvinylpyrrolidone (PVP, average M_w ~55000, Aldrich) was added to the solutions. The surfactant was added to the rare-earth nitrates solutions before precipitation. The freshly precipitated gel was diluted with 10 ml dH_2O and left stirring for 15 min. The solution was transferred into a 100 ml Teflon autoclave and placed under microwave irradiation for 2 hours at 200°C using a microwave digestion laboratory device Speedwave Four (2.45 GHz, 1 kW maximum output power, Berghof, Germany). The resulting solution was cooled, centrifuged using a Heraeus Multifuge X1 (Thermo Fisher Scientific, USA) and washed several times with dH_2O. The resulting powder was redispersed in dH_2O.

Characterization of Nd^{3+}:LaF_3 NPs

The X-Ray Diffraction (XRD) analysis of the Nd^{3+}:LaF_3 NPs synthesized using HTMW treatment was performed as earlier [16]. The NPs demonstrate pure and highly crystalline LaF_3 phase.

The morphology of the Nd^{3+}:LaF_3 NPs was studied by means of high-resolution transmission electron microscopy (HR TEM) using the Titan 200 instrument (FEI, USA) with a field emission gun operating at 200 kV. The sample was prepared by dropping NPs colloidal solution onto a formvar or holey carbon coated copper (grid 3 mm in diameter) followed by the evaporation of the solvent.

Hydrodynamic sizes of Nd^{3+}:LaF_3 NPs in dH_2O were determined by multiangle spectrometer of dynamic light scattering Photocor Complex (Photocor, Russia). ζ-potential measurements were determined using a Zetasizer Nano ZS (Malvern Instruments, UK) analyzer in dH_2O at 25 °C. All measurements were performed in triplicate.

The absorption spectra of Nd^{3+}:LaF_3 NPs were recorded on a spectrophotometer U-3400 (Hitachi, Japan).

Confocal microscopy

Intracellular Nd^{3+}:LaF_3 NPs distribution was studied using human monocytic cell line derived from an acute monocytic leukaemia patient (THP-1). THP-1 cells were cultured in Roswell Park Memorial Institute Medium (RPMI-1640) containing 10% fetal bovine serum (FBS) at 37°C in 5% CO_2. Cells were sub-cultured every seventh day. For confocal microscopy experiments, monocytic cells were differentiated into macrophage-like cells using Concanavalin A (ConA). Cells were seeded at a density of 100 000 cells/cm^2 on glass bottom dishes with cell culture medium containing 30 μg/ml ConA for three days. During this time, cells attach to the glass bottom and develop macrophage-like morphology. Next, macrophages were incubated with Nd^{3+}:LaF_3 NPs (100 μg for 500 000 cells) for 2÷72 hours.

For microscopy the cells were finally washed twice with pre-warmed phosphate buffered saline (PBS). For visualization of lysosomes the washed cells were incubated in PBS with 50 nM LysoTracker Green DND-26 (Molecular Probes®) during 20 min at 37°C in 5% CO_2. The nuclei were stained in PBS with 2 nM Hoechst 33342 (Molecular Probes®) during 10 min at 37°C in 5% CO_2. To acquire images a laser scanning microscope LSM- 710-NLO (Zeiss, Germany) was used. The 63× oil Plan-Apochromat objective with numerical aperture (NA) of 1.4 was used.

The upconversion luminescence of Nd^{3+}:LaF_3 NPs were excited with a pulse femtosecond Chameleon Ultra II laser system (Coherent, USA), tunable in the 690÷1060 nm range, 80 MHz pulse laser, 140 fs pulse width.

The power density produced by the scanning laser beam emerging from the objective lens in the object plane was calculated as follows. The size of this focusing laser spot, assuming uniform illumination, is a function of the excitation wavelength (λ_{exc}) and the parameter NA of the objective:

$$S_{spotsize} = 1.22\lambda_{exc}/_{NA}$$

Thus, for a wavelength of 738 nm and a 63xOil objective with aperture NA = 1.4, the spot size was ~640 nm, for a wavelength of 795 nm ~690 nm. Accordingly, for the 1% laser power or 1 mW measured at the output of the objective with the LabMax-TO laser power meter (Coherent, USA) the power densities are 0.313 MW/cm^2 (for 738 nm laser) and 0.263 MW/cm^2 (for 795 nm laser). The dose of laser radiation with a single scan at speed 2.55 μs/pix was 0.80 J/cm^2 for 738 nm laser and 0.67 J/cm^2 for 795 nm laser, respectively.

The luminescence emission was detected by the 32 channel GaAsP detector in VIS spectral range 400÷750 nm. To discriminate between Nd^{3+} upconversion luminescence and fluorescence of LysoTrackerGreen DND-26 or Hoechst 33342, "Online Fingerprint" mode was used. For this purpose, the upconversion luminescence spectra of the Nd^{3+}:LaF_3 NPs and fluorescence of LysoTrackerGreen DND-26 or Hoechst 33342 at the same two photon excitation were detected beforehand. As fluorescence of LysoTrackerGreen DND-26 or Hoechst 33342 has gently sloping broad line in the range 400-600 nm, and upconversion luminescence Nd^{3+} ions has characteristic comb of narrow peaks, then the total fluorescence corresponding to each pixel can be decomposed into the components [17].

The Nd^{3+}:LaF_3 NPs upconversion luminescence intensity dependence from pump power

The Nd^{3+}:LaF_3 NPs upconversion luminescence intensity dependence in VIS spectral range 400÷750 nm on 140 fs pulse width 80 MHz pulse laser pump power

varying in 0.1÷5.5 MW/cm^2 at 738 and 795 nm wavelengths was measured using 32 channel GaAsP photomultiplier detector in LSM-710-NLO. The obtained spectral images were used to plot the intensity dependences of the upconversion luminescence for individual Nd^{3+} electronic transitions.

Transmission electron microscopy (TEM)

For TEM experiments, THP-1 cells were differentiated into macrophage-like cells using phorbol 12-myristate 13-acetate (PMA). The cells were seeded at a density of 50 000 cells/cm^2 in cell culture medium in the presents of PMA at final concentration of 200 nM for differentiation for three days. After differentiation, macrophages were incubated with Nd^{3+}:LaF_3 NPs (100 µg for 100 000 cells) for 48 hours.

Cells were then gently washed with pre-warmed PBS, trypsinized for 5 min at 37°C in 5% CO_2 and fixed with 4% methanol-free paraformaldehyde (PFA) overnight in the fridge to produce pellets. Then the pellets were washed three times with double distilled water (ddH_2O) and 0.1 M cacodylate buffer. For TEM contrast, the pellets were stained with 2% osmium tetroxide (OsO_4) and 1.5% potassium ferricyanide for 1 hour. Next, the pellets were washed with ddH_2O and gradually dehydrated using an ethanol gradient (20%, 40%, 60%, 70%, 80%, 90%, 95%, 100% (3x)) for 5 min. The pellets were embedded to epoxy resin (EPON 812) according to procedures described in the manufacturer's protocol. Resin blocks were cured in the oven for 72 hours, trimmed with a razor blade and sectioned in 100 nm sections using an ultramicrotome. Acquired thin sections were imaged using JEOL 2000FX at 80 kV.

Results and discussion

Nd^{3+}-doped LaF_3 nanoparticles are synthesized via microwave assisted hydrothermal reaction. HR TEM results show that synthesized Nd^{3+}:LaF_3NPs are crystalline with elongated or hexagonal form and a size around 15 to 20 nm (Inset on the Fig. 2). The hydrodynamic size of the particles in colloid is amounted to be 70 nm. The colloidal solution remains stable more than 6 months without noticeable precipitation, because of PVP envelope for each NP. The ζ-potential of these NPs was 13.7±0.9 mV, which is similar to the results obtained for other PVP-functionalized nanoparticles.

The energy level scheme for the trivalent neodymium ions in a Nd^{3+} LaF_3crystal is plotted on the base of literature data (Fig. 1) [18, 19].

The absorption spectra, NIR luminescence spectra of the Nd^{3+}:LaF_3 NPs aqueous colloidal solution, obtained by excitation with 800 nm wavelength at 1 W/cm^2 of continuous wave (CW) laser, and upconversion luminescence obtained with 738 nm and 795 nm wavelengths of femtosecond laser, at 1 MW/cm^2 average power density are presented in Fig. 2.

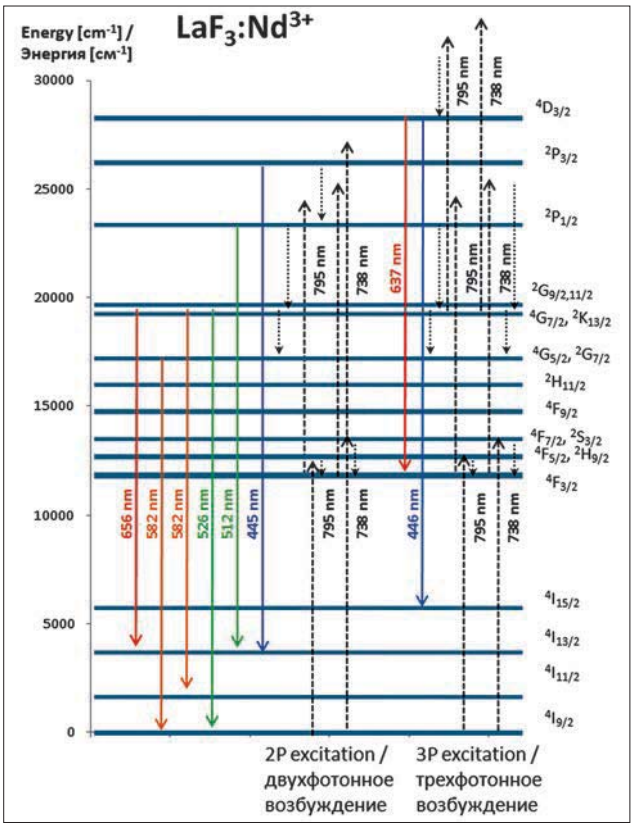

Fig. 1. The energy level diagram of Nd^{3+} ions in the LaF_3 host matrix
Рис. 1. Диаграмма уровней энергии иона Nd^{3+} в допирующей матрице LaF_3

At both types of excitation, 738 nm and 795 nm, the upconversion luminescence has almost equal intensity and shows different spectral bands of Nd^{3+} (Fig. 2). The laser excitation at 795 nm induces the $^4I_{9/2}\rightarrow{}^2H_{9/2}$, $^4F_{5/2}$ transition of Nd^{3+} ions, followed by nonradiative relaxation to the $^4F_{3/2}$ metastable state. The laser excitation at 738 nm induces the $^4I_{9/2}\rightarrow{}^4F_{7/2}$, $^2S_{3/2}$ transition of Nd^{3+} ions, followed by nonradiative relaxation to the $^4F_{3/2}$ metastable state. At a sufficient power density, the next photon induced absorption transition from the excited $^4F_{3/2}$ state (exited state absorption process, ESA). In addition, there is a resonance cross-relaxation ($^4F_{3/2}\rightarrow{}^4I_{15/2}$; $^4I_{9/2}\rightarrow{}^4I_{15/2}$) transitions from this state, but it is not involved in the upconversion. Thus, the $^2P_{1/2}$ level is excited, followed by nonradiative relaxation to the $^4G_{7/2}$, $^2K_{13/2}$ metastable state and then to the $^4G_{5/2}$ state. When the third photon is absorbed, the levels higher than $^2P_{3/2}$ are populated (Fig. 1).

The upconversion luminescence intensity I_{vis} in the VIS spectral range depends on the pumping power I_p as $I_{vis} \propto I_p^n$ where n is the number of NIR photons which are absorbed for emission of one photon in the VIS range [20].

However, in practice, deviations from this dependence can be observed. The slope of the dependence

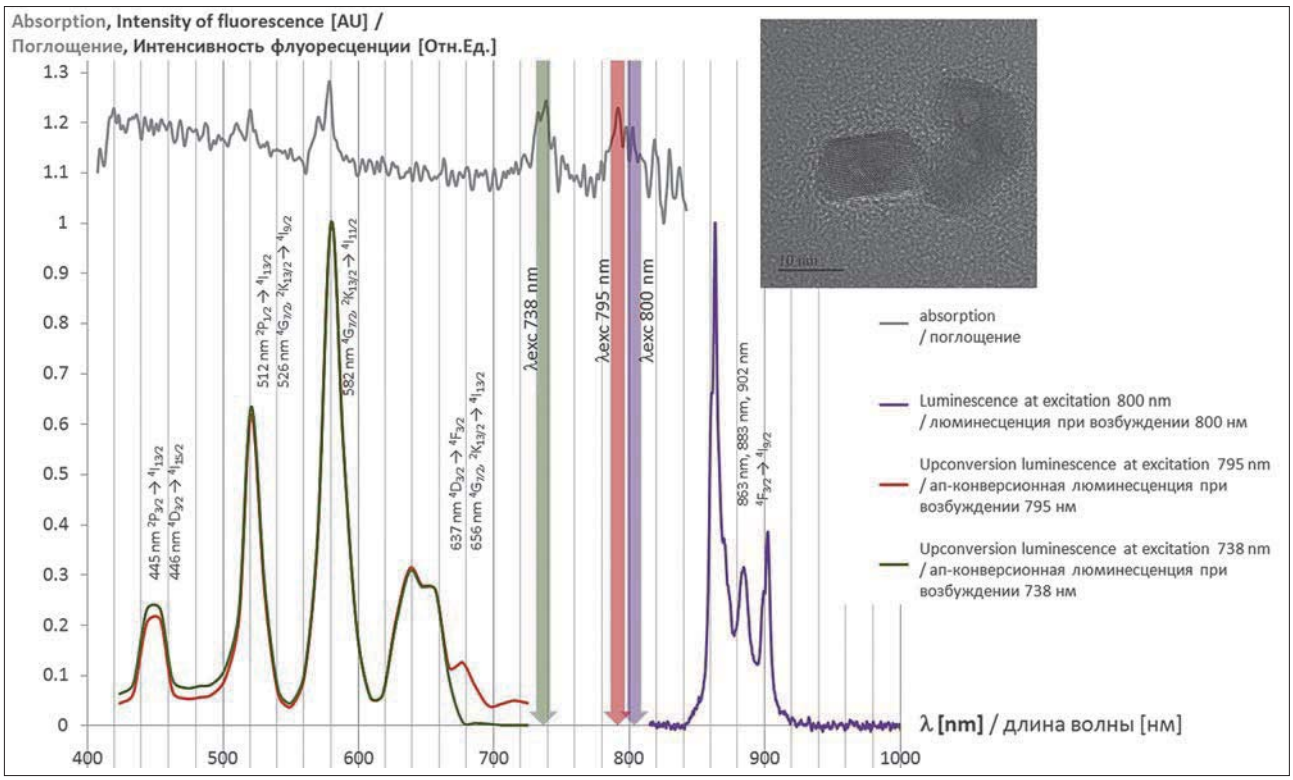

Fig. 2. Nd^{3+}:LaF_3NPs spectra: absorption, upconversion luminescence at fs pulsed excitation 738 nm and 795 nm, NIR luminescence at excitation 800 nm; on the inset is HRTEM image of Nd^{3+}:LaF_3 NPs
Рис. 2. Спектры НЧ Nd^{3+}:LaF_3: поглощение, ап-конверсионная люминесценция при фемтосекундном импульсном возбуждении 738 нм и 795 нм, БИК люминесценция при возбуждении 800 нм; на вставке – высокоразрешающая просвечивающая электронная микроскопия НЧ Nd^{3+}:LaF_3

of the upconversion luminescence intensity on the pump power is determined by the competition between relaxation processes and upconversion during the population of excited states of the acceptor. The slope depends on energy transfer to impurity ions, energy migration among donor ions, the inhomogeneous distribution of doping ions in the matrix, and temperature [21]. In our experiments, the dependence of the intensity of the transition $^2P_{3/2}\rightarrow{}^4I_{13/2}$ and $^4D_{3/2}\rightarrow{}^4I_{15/2}$ (420÷460 nm), $^2P_{1/2}\rightarrow{}^4I_{13/2}$ and $^4G_{7/2}$, $^2K_{13/2}\rightarrow{}^4I_{9/2}$ (500÷550 nm), $^4G_{5/2}\rightarrow{}^4I_{9/2}$ and $^4G_{7/2}$, $^2K_{13/2}\rightarrow{}^4I_{11/2}$ (560÷600 nm), $^4D_{3/2}\rightarrow{}^4F_{3/2}$ and $^4G_{7/2}$, $^2K_{13/2}\rightarrow{}^4I_{13/2}$ (620÷660 nm) on the incident pump power (in the range 0.5÷2 MW/cm²) gives values of 1.5, 1.5, 1.3 and 1.5 for *n*, respectively, which indicate two-photon upconversion processes (Fig. 3).

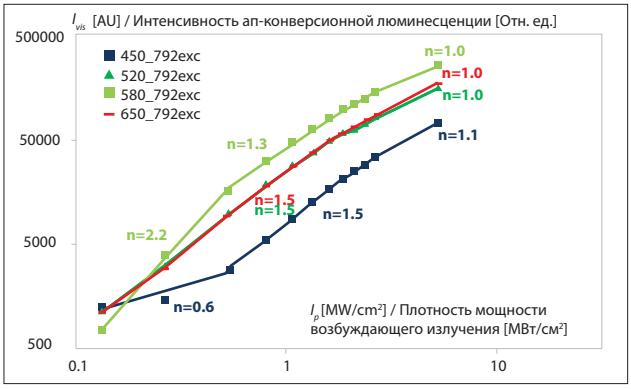

Fig. 3. The pumping power dependence of Nd^{3+}:LaF_3 NPs upconversion luminescence intensity under 795 nm excitation
Рис. 3. Зависимость интенсивности ап-конверсионной люминесценции НЧ Nd^{3+}:LaF_3 от плотности мощности накачки при возбуждении 795 нм

The exponent *n*, if smaller than unity, is related to deactivation processes. The upconversion efficiency for studied NPs is far from ideal, but using a pulsed laser for excitation makes it possible to produce images without visible cell structures damage. Similar orders of power density (35 kW/cm² ÷ 3.6 MW/cm²) of CW 730 nm laser was used to obtain two-photon, three-photon image and four-photon image of Nd^{3+}-doped NPs [15]. Fast scanning speeds can cause artifacts in fluorescence imaging because of long lifetimes from Nd^{3+} NPs. The authors of this article noted the streaking artifacts at the scan speed more than 100 μs/pixel. We use scan speed 2.55 μs/pixel to reduce the laser heating effects on cells, and at such scan speed the streaking effect was not observed.

The images in the Fig. 4 are obtained at the simultaneous excitation of the LysoTrackerGreen DND-26 or Hoechst 33342 and Nd^{3+}:LaF_3 NPs by laser 795 nm with a power density 1 MW/cm².

Confocal microscopy indicates cellular uptake of Nd^{3+}:LaF_3 NPs. After incubation of live cells with NPs, it

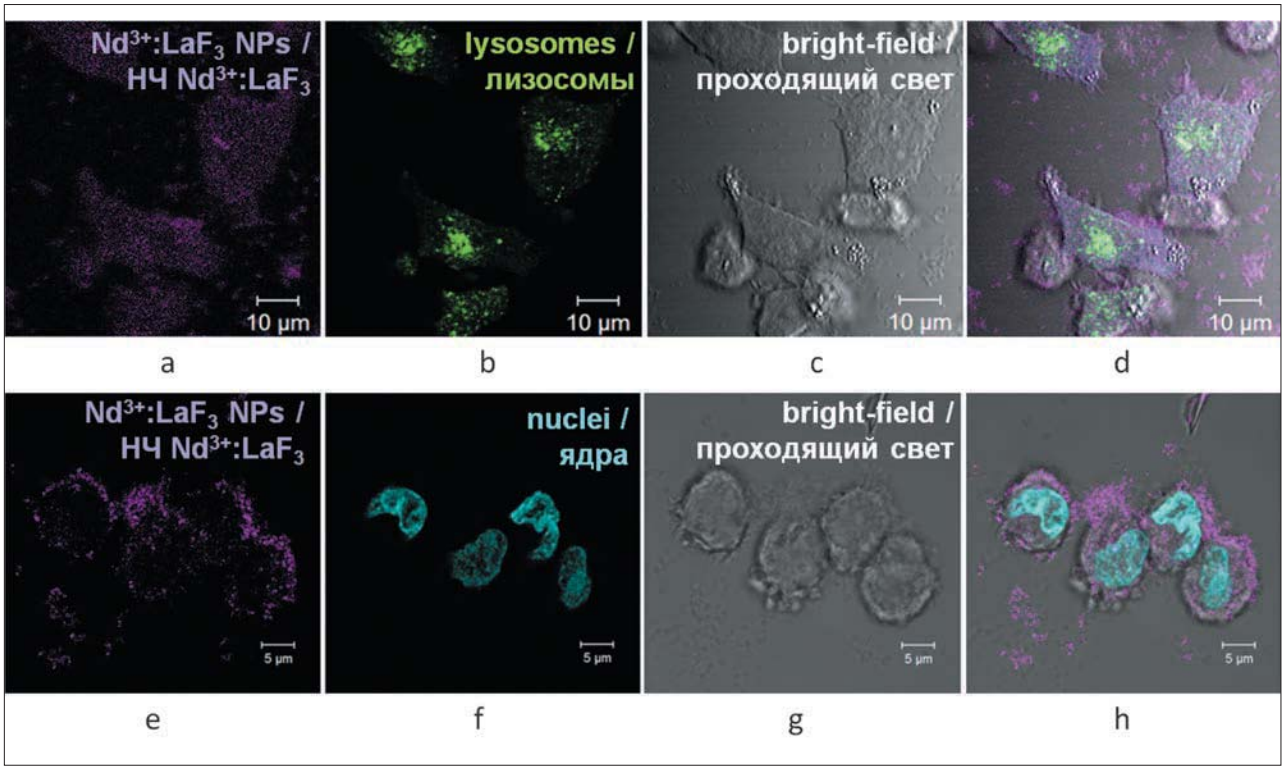

Fig. 4. Confocal fluorescent images of intracellular distribution of Nd^{3+}:LaF_3 NPs on THP-1 cells acquired at excitation wavelengths of 795 nm by separation into individual channels after linear unmixing of spectral image (on the images a, b, c and d the lysosomes are additionally stained, on the images e, f, g and h the nuclei are additionally stained):
a – deconvoluted from the spectral image signal of upconversion luminescence from the Nd^{3+}:LaF_3 NPs;
b – deconvoluted from the spectral image signal from lysosomes stained with LysoTrackerGreen DND-26;
c – bright-field micrographs of the cell taken under visible light;
d – superimposing of a, b and c images;
e – deconvoluted from the spectral image signal of upconversion luminescence from the Nd^{3+}:LaF_3 NPs;
f – deconvoluted from the spectral image signal from nuclei stained with Hoechst 3334;
g – bright-field micrographs of the cell taken under visible light;
h – superimposing of e, f and g images

Рис. 4. Конфокальное флуоресцентное изображение внутриклеточного распределения НЧ Nd^{3+}:LaF_3 в клетках THP-1, полученное при возбуждении 795 нм путем разделения на отдельные каналы после линейного разложения спектрального изображения (на изображениях a, b, c и d – клетки дополнительно окрашены на лизосомы; на изображениях e, f, g и h – клетки дополнительно окрашены на ядра):
a – сигнал ап-конверсионной люминесценции НЧ Nd^{3+}:LaF_3, выделенный из спектрального изображения;
b – выделенный из спектрального изображения сигнал лизосомального красителя LysoTrackerGreen DND-26;
c – изображение клеток в проходящем свете;
d – наложение изображений a, b и c;
e – сигнал ап-конверсионной люминесценции НЧ Nd^{3+}:LaF_3, выделенный из спектрального изображения;
f – выделенный из спектрального изображения сигнал ядерного красителя Hoechst 3334;
g – изображение клеток в проходящем свете;
h – наложение изображений e, f и g

is confirmed that NPs are located inside the cells. The fluorescence obtained from NPs coincides quite well with the signal from the stained lysosomes. However, it is also seen that some NPs are attached to the inner and outer membranes. Also, some of the bigger aggregates, not associated with the uptake, are visible. From the confocal microscopy images it is obvious that the Nd^{3+}:LaF_3 NPs are located in macrophage-like THP-1 cells closer to the cytoplasm membrane, but also occur throughout the cytoplasm. In the cytoplasm, NPs formed clusters, feasibly, are occur in small spherical endosome-like organelles, but not all organelles containing NPs are stained as lysosomes. Some of the NPs are attached to the surface of the cells from the outside, and in addition, the NPs aggregates at the bottom of the Petri dish can be seen. Perhaps such a distribution of NPs is associated with their positive surface charge.

A more detailed Nd^{3+}:LaF_3 NPs distribution within the THP-1 cell can be seen on the TEM image (Fig. 5). The images clearly indicate uptake of NPs into vesicles and their aggregation in the live cells. On the right image on the Fig. 5 protrusion of the plasma membrane for phagocytosis is observed. TEM indicate the presence of NPs in the endosomes and on the plasma membrane outside the cell.

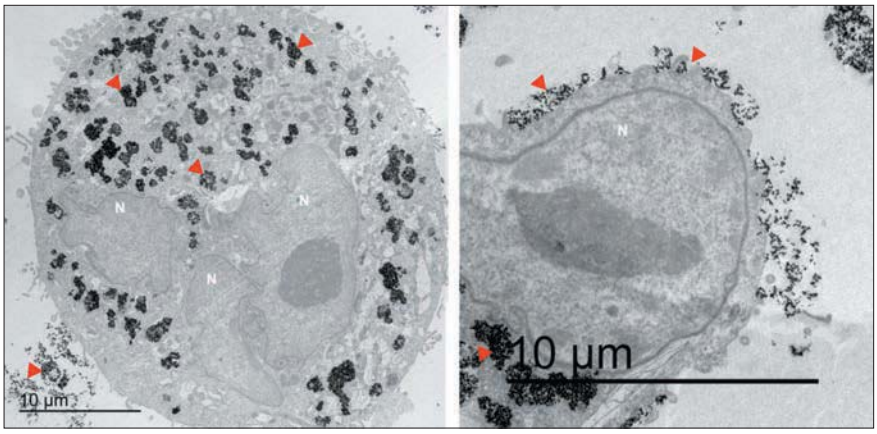

Fig. 5. TEM images of differentiated THP-1 cells after being exposed to Nd^{3+}:LaF_3 NPs for 48 hour: white letter N mark nuclei, red arrows indicate NPs
Рис. 5. Просвечивающая электронная микроскопия дифференцированных клеток THP-1 после инкубации с НЧ Nd^{3+}:LaF_3 в течение 48 ч: ядра отмечены белыми буквами N, НЧ указаны красными стрелками

Cellular uptake of NPs is strongly dependent on their surface charge. It has been shown that positively charged NPs are more permeable for cells [22]. Studied PVP enveloped Nd^{3+}:LaF_3 NPs show a small positive charge. In general, hydrophilic sodium fluoride-based NPs doped with lanthanide ions have very low toxicity to granulocytes from the phagocytosis point of view [23]. Their uptake by macrophage-like cells THP-1 was observed from two hours to three days.

Conclusion

Accumulation of Nd^{3+}:LaF_3 NPs in living cells was demonstrated by detecting upconversion luminescence with laser scanning confocal microscopy. Despite the low quantum yields of the VIS upconversion luminescence for the Nd^{3+}:LaF_3 NPs in aqueous colloidal solutions, when pulse excitation is used, it is possible to reliably record the VIS signal of Nd^{3+}:LaF_3 NPs upconversion luminescence at 1 MW/cm^2 power density, still not destroying the cells. The excitation at 738 nm, induces the $^4I_{9/2} \rightarrow {}^4F_{7/2}$, $^2S_{3/2}$ transition of Nd^{3+} ions and 795 nm, induces the $^4I_{9/2} \rightarrow {}^2H_{9/2}$, gives almost equal the upconversion luminescence intensity from the Nd^{3+} bands.

This work was supported by the Russian Science Foundation [grant number 16-12-10077], the Marie Curie Actions FP7-PEOPLE-2013-IRSES [grant number 612620] and the European Regional Development Fund (TK141 "Advanced materials and high-technology devices for energy recuperation systems"). HR TEM measurements were supported by projects IUT2-24 and IUT20-54 of the Estonian Ministry of Education and Research.

ЛИТЕРАТУРА

1. Escudero A., Carrillo-Carrión C., Zyuzin M.V., Parak W.J. Luminescent rare-earth-based nanoparticles: a summarized overview of their synthesis, functionalization, and applications // Top Curr Chem (Cham). – 2016. – Vol. 374(4). – P. 48. https://doi.org/10.1007/s41061-016-0049-8.
2. Ma D., Xu X., Hu M., et al. Rare-earth-based nanoparticles with simultaneously enhanced near-infrared (NIR)-visible (Vis) and NIR-NIR dual-conversion luminescence for multimodal imaging // Chem Asian J. – 2016. – Vol. 11(7). – P. 1050-1058. http://dx.doi.org/10.1002/asia.201501456.
3. Li X., Wang R., Zhang F., et al. Nd^{3+} Sensitized up/down converting dual-mode nanomaterials for efficient *in-vitro* and *in-vivo* bioimaging excited at 800 nm // Sci. Rep. – 2013. – Vol. 3. – P. 3536. http://dx.doi.org/10.1038/srep03536.
4. Wang Z., Zhang P., Yuan Q., et al. Nd^{3+}-sensitized $NaLuF_4$ luminescent nanoparticles for multimodal imaging and temperature sensing under 808 nm excitation // Nanoscale. – 2015. – Vol. 7(42). – P. 17861-17870. http://dx.doi.org/10.1039/C5NR04889C.

REFERENCES

1. Escudero A., Carrillo-Carrión C., Zyuzin M.V., Parak W.J. Luminescent rare-earth-based nanoparticles: a summarized overview of their synthesis, functionalization, and applications, *Top Curr Chem (Cham)*, 2016, Vol. 374(4), p. 48. Available at: https://doi.org/10.1007/s41061-016-0049-8
2. Ma D., Xu X., Hu M., Wang J., Zhang Z., Yang J., Meng L. Rare-earth-based nanoparticles with simultaneously enhanced near-infrared (NIR)-visible (Vis) and NIR-NIR dual-conversion luminescence for multimodal imaging, *Chem Asian J*, 2016, Vol. 11(7), pp. 1050-1058. Available at: http://dx.doi.org/10.1002/asia.201501456
3. Li X., Wang R., Zhang F., Zhou L., Shen D., Yao C., Zhao D. Nd3+ Sensitized up/down converting dual-mode nanomaterials for efficient *in-vitro* and *in-vivo* bioimaging excited at 800 nm, *Sci. Rep.*, 2013, Vol. 3, p. 3536. Available at: http://dx.doi.org/10.1038/srep03536
4. Wang Z., Zhang P., Yuan Q., Xu X., Lei P., Liu X., Su Y., Dong L., Feng J., Zhang H. Nd^{3+}-sensitized $NaLuF_4$ luminescent nanoparticles for multimodal imaging and temperature sensing under 808 nm excitation, *Nanoscale*, 2015, Vol. 7(42), pp. 17861-17870. Available at: http://dx.doi.org/10.1039/C5NR04889C

5. Zhong Y., Tian G., Gu Z., et al. Elimination of photon quenching by a transition layer to fabricate a quenching-shield sandwich structure for 800 nm excited upconversion luminescence of Nd^{3+}-sensitized nanoparticles // Adv. Mater. – 2014. – Vol. 26(18). – P. 2831-2837. http://dx.doi.org/10.1002/adma.201304903.
6. Zhan Q., Wang B., Wen X., He S. Controlling the excitation of upconverting luminescence for biomedical theranostics: neodymium sensitizing // Opt. Mater. Express. – 2016. – Vol. 6. – P. 1011-1023. https://doi.org/10.1364/OME.6.001011.
7. Kushida T., Marcos H.M., Geusic J.E. Laser transition cross section and fluorescence branching ratio for Nd^{3+} in yttrium aluminum garnet // Phys. Rev. – 1968. – Vol. 167. – P. 289-291. https://doi.org/10.1103/PhysRev.167.289.
8. Xu B., Zhang X., Huang W., et al. Nd^{3+} sensitized dumbbell-like upconversion nanoparticles for photodynamic therapy application // *J. Mater. Chem.* B. – 2016. – Vol. 4. – P. 2776-2784. http://dx.doi.org/10.1039/C6TB00542J.
9. Wang Y.F., Liu G.Y., Sun L.D., et al. Nd(3+)-sensitized upconversion nanophosphors: efficient in vivo bioimaging probes with minimized heating effect // ACS Nano. – 2013. – Vol. 7. – P. 7200-7206. doi:10.1021/nn402601d.
10. Qin Q.-S., Zhang P.-Z., Sun L.-D., et al. Ultralow-power near-infrared excited neodymium-doped nanoparticles for long-term in vivo bioimaging // Nanoscale. – 2017. – Vol. 9. – P. 4660-4664. http://dx.doi.org/10.1039/C7NR00606C.
11. Rocha U., Hu J., Rodriguez E.M., et al. Subtissue Imaging and Thermal Monitoring of Gold Nanorods through Joined Encapsulation with Nd-Doped Infrared-Emitting Nanoparticles // Small. – 2016. – Vol. 12. – P. 5394-5400. http://dx.doi.org/10.1002/smll.201600866.
12. Pichaandi J., Boyer J.-C., Delaney K.R., van Veggel F.C.J.M. Two-photon upconversion laser (scanning and wide-field) microscopy using Ln^{3+}-doped $NaYF_4$ upconverting nanocrystals: a critical evaluation of their performance and potential in bioimaging // J. Phys. Chem. C. – 2011. – Vol. 115. – P. 19054-19064. doi:10.1021/jp206345j.
13. Zhan Q., He S., Qian J., et al. Optimization of optical excitation of upconversion nanoparticles for rapid microscopy and deeper tissue imaging with higher quantum yield // Theranostics. – 2013. – Vol. 3. – P. 306-316. doi:10.7150/thno.6007.
14. Wu R., Zhan Q., Liu H., et al. Optical depletion mechanism of upconverting luminescence and its potential for multi-photon STED-like microscopy // Opt. Express. – 2015. – Vol. 23. – P. 32401-32412. https://doi.org/10.1364/OE.23.032401.
15. Wang B., Zhan Q., Zhao Y., et al. Visible-to-visible four-photon ultrahigh resolution microscopic imaging with 730-nm diode laser excited nanocrystals // Opt. Express. – 2016. – Vol. 24(2). – A302-A311. https://doi.org/10.1364/OE.24.00A302.
16. Vanetsev A., Kaldvee K., Puust L., et al. Relation of crystallinity and fluorescent properties of LaF_3:Nd^{3+} nanoparticles synthesized with different water-based techniques. // Chemistry Select. – 2017. – Vol. 2. – P. 4874-4881. http://dx.doi.org/10.1002/slct.201701075.
17. Shcherbakov A.B., Zholobak N.M., Baranchikov A.E., et al. Cerium fluoride nanoparticles protect cells against oxidative stress // Mater Sci. Eng. C Mater Biol. Appl. – 2015. – Vol. 50. – P. 151-159. https://doi.org/10.1016/j.msec.2015.01.094.
18. Carnall W.T., Crosswhite Hannah, Crosswhite H.M. Energy level structure and transition probabilities in the spectra of the trivalent lanthanides in LaF_3. – United States, 1978. doi:10.2172/6417825.
19. Carnall W.T., Goodman G.L., Rajnak K., Rana R.S. A systematic analysis of the spectra of the lanthanides doped into single crystal LaF_3 // J. Chem. Phys. – 1989. – Vol. 90. – P. 3443. http://dx.doi.org/10.1063/1.455853.

5. Zhong Y., Tian G., Gu Z., Yang Y., Gu L., Zhao Y., Ma Y., Yao J. Elimination of photon quenching by a transition layer to fabricate a quenching-shield sandwich structure for 800 nm excited upconversion luminescence of Nd^{3+}-sensitized nanoparticles, *Adv. Mater.*, 2014, Vol. 26(18), pp. 2831-2837. Available at: http://dx.doi.org/10.1002/adma.201304903
6. Zhan Q., Wang B., Wen X., He S. Controlling the excitation of upconverting luminescence for biomedical theranostics: neodymium sensitizing, *Opt. Mater. Express*, 2016, Vol. 6, pp. 1011-1023. Available at: https://doi.org/10.1364/OME.6.001011
7. Kushida T., Marcos H.M., Geusic J.E. Laser transition cross section and fluorescence branching ratio for Nd^{3+} in yttrium aluminum garnet, *Phys. Rev.*, 1968, Vol. 167, pp. 289-291. Available at: https://doi.org/10.1103/PhysRev.167.289
8. Xu B., Zhang X., Huang W., Yang Y., Ma Y., Gu Z., Zhai T., Zhao Y. Nd3+ sensitized dumbbell-like upconversion nanoparticles for photodynamic therapy application, *J. Mater. Chem. B.*, 2016, Vol. 4, pp. 2776-2784. Available at: http://dx.doi.org/10.1039/C6TB00542J
9. Wang Y.F., Liu G.Y., Sun L.D., Xiao J.W., Zhou J.C., Yan C.H. Nd(3+)-sensitized upconversion nanophosphors: efficient in vivo bioimaging probes with minimized heating effect, *ACS Nano*, 2013, Vol. 7, pp. 7200-7206. doi:10.1021/nn402601d
10. Qin Q.-S., Zhang P.-Z., Sun L.-D., Shi S., Chen N.-X., Dong H., Zheng X.-Y., Li L.-M. and Yan C.-H. Ultralow-power near-infrared excited neodymium-doped nanoparticles for long-term in vivo bioimaging, *Nanoscale*, 2017, Vol. 9, pp. 4660-4664. Available at: http://dx.doi.org/10.1039/C7NR00606C
11. Rocha U., Hu J., Rodriguez E.M., Vanetsev A.S., Rähn M., Sammelselg V., Orlovskii Y.V., García Sole J., Jaque D., Ortgies D.H. Subtissue Imaging and Thermal Monitoring of Gold Nanorods through Joined Encapsulation with Nd-Doped Infrared-Emitting Nanoparticles, *Small*, 2016, Vol. 12, pp. 5394-5400. Available at: http://dx.doi.org/10.1002/smll.201600866
12. Pichaandi J., Boyer J.-C., Delaney K.R., van Veggel F.C.J.M. Two-photon upconversion laser (scanning and wide-field) microscopy using Ln3+-doped NaYF4 upconverting nanocrystals: a critical evaluation of their performance and potential in bioimaging, *J. Phys. Chem. C.*, 2011, Vol. 115, pp. 19054-19064. doi:10.1021/jp206345j
13. Zhan Q., He S., Qian J., Cheng H., Cai F. Optimization of optical excitation of upconversion nanoparticles for rapid microscopy and deeper tissue imaging with higher quantum yield, *Theranostics*, 2013, Vol. 3, pp. 306-316. doi:10.7150/thno.6007
14. Wu R., Zhan Q., Liu H., Wen X., Wang B., He S. Optical depletion mechanism of upconverting luminescence and its potential for multi-photon STED-like microscopy, *Opt. Express*, 2015, Vol. 23, pp. 32401-32412. Available at: https://doi.org/10.1364/OE.23.032401
15. Wang B., Zhan Q., Zhao Y., Wu R., Liu J., He S. Visible-to-visible four-photon ultrahigh resolution microscopic imaging with 730-nm diode laser excited nanocrystals, *Opt. Express*, 2016, Vol. 24(2), pp. A302-A311. Available at: https://doi.org/10.1364/OE.24.00A302
16. Vanetsev A., Kaldvee K., Puust L., Keevend K., Nefedova A., Fedorenko S., Baranchikov A., Sildos I., Rahn M., Sammelselg V., Orlovskii Y. Relation of crystallinity and fluorescent properties of LaF3:Nd^{3+} nanoparticles synthesized with different water-based techniques, *Chemistry Select*, 2017, Vol. 2, pp. 4874-4881. Available at: http://dx.doi.org/10.1002/slct.201701075
17. Shcherbakov A.B., Zholobak N.M., Baranchikov A.E., Ryabova A.V., Ivanov V.K. Cerium fluoride nanoparticles protect cells against oxidative stress, *Mater Sci. Eng. C Mater Biol. Appl.*, 2015, Vol. 50, pp. 151-159. Available at: https://doi.org/10.1016/j.msec.2015.01.094
18. Carnall W.T., Crosswhite Hannah, Crosswhite H.M. *Energy level structure and transition probabilities in the spectra of the trivalent lanthanides in LaF3*. United States, 1978. doi:10.2172/6417825
19. Carnall W.T., Goodman G.L., Rajnak K., Rana R.S. A systematic analysis of the spectra of the lanthanides doped into single crystal LaF3, *J. Chem. Phys.*, 1989, Vol. 90, p. 3443. Available at: http://dx.doi.org/10.1063/1.455853

20. Pollnau M., Gamelin D.R., Luthi S.R., et al. Power dependence of upconversion luminescence in lanthanide and transition-metal-ion systems // Phys. Rev. B. – 2000. – Vol. 61. – P. 3337-3346. https://doi.org/10.1103/PhysRevB.61.3337.
21. Jacinto C., Oliveira S.L., Catunda T., et al. Upconversion effect on fluorescence quantum efficiency and heat generation in Nd^{3+}-doped materials // Opt. Express. – 2005. – Vol. 13. – P. 2040-2046. https://doi.org/10.1364/OPEX.13.002040.
22. Fröhlich E. The role of surface charge in cellular uptake and cytotoxicity of medical nanoparticles // Int. J. Nanomedicine. – 2012. – Vol. 7. – P. 5577-5591. https://doi.org/10.2147/IJN.S36111.
23. Sojka B., Liskova A., Kuricova M., et al. The effect of core and lanthanide ion dopants in sodium fluoride-based nanocrystals on phagocytic activity of human blood leukocytes // J. Nanopart. Res. – 2017. – Vol. 19. – P. 68. https://doi.org/10.1007/s11051-017-3779-9.

20. Pollnau M., Gamelin D.R., Luthi S.R., Gudel H.U., Hehlen M.P. Power dependence of upconversion luminescence in lanthanide and transition-metal-ion systems, *Phys. Rev. B.*, 2000, Vol. 61, pp. 3337-3346. Available at: https://doi.org/10.1103/PhysRevB.61.3337
21. Jacinto C., Oliveira S.L., Catunda T., Andrade A.A., Myers J.D., Myers M.J. Upconversion effect on fluorescence quantum efficiency and heat generation in Nd^{3+}-doped materials, *Opt. Express*, 2005, Vol. 13, pp. 2040-2046. Available at: https://doi.org/10.1364/OPEX.13.002040
22. Fröhlich E. The role of surface charge in cellular uptake and cytotoxicity of medical nanoparticles, *Int. J. Nanomedicine*, 2012, Vol. 7, pp. 5577-5591. Available at: https://doi.org/10.2147/IJN.S36111
23. Sojka B., Liskova A., Kuricova M., Banski M., Misiewicz J., Dusinska M., Horvathova M., IlavskaS., Szabova M., Rollerova E., Podhorodecki A., Tulinska J. The effect of core and lanthanide ion dopants in sodium fluoride-based nanocrystals on phagocytic activity of human blood leukocytes, *J. Nanopart. Res.*, 2017, Vol. 19, p. 68. Available at: https://doi.org/10.1007/s11051-017-3779-9